

Integrated micromechanical cantilever magnetometry of $\text{Ga}_{1-x}\text{Mn}_x\text{As}$

J. G. E. Harris and D. D. Awschalom^{a)}

Department of Physics, University of California, Santa Barbara, California 93106

F. Matsukura and H. Ohno

Laboratory for Electronic Intelligent Systems, Research Institute of Electrical Communications, Tohoku University, Aoba-ku, Sendai 980-8577, Japan

K. D. Maranowski and A. C. Gossard

Department of Electrical and Computer Engineering, University of California, Santa Barbara, California 93106

(Received 11 March 1999; accepted for publication 29 June 1999)

We have developed a technique for fabricating submicron GaAs micromechanical cantilevers into which lithographically patterned samples grown by molecular beam epitaxy or evaporative deposition are integrated. The torque sensitivity of the 100-nm-thick cantilevers makes them ideal for torsional magnetometry of nanometer-scale, anisotropic samples. We present measurements on samples of the ferromagnetic semiconductor $\text{Ga}_{1-x}\text{Mn}_x\text{As}$ at temperatures from 350 mK to 65 K and in fields from 0 to 8 T. By measuring the shift in the resonant frequency of the cantilevers, we demonstrate a moment sensitivity of $3 \times 10^6 \mu_B$ at 0.1 T, an improvement of nearly five orders of magnitude upon existing torsional magnetometers. © 1999 American Institute of Physics. [S0003-6951(99)03934-0]

Torsional magnetometry provides a powerful approach to measuring the magnetic properties of small samples over a wide range of applied magnetic fields and temperatures. Torsional magnetometers rely upon the torque between the magnetic moment of a sample and the applied field to produce a signal, which can be detected either as a displacement of a torsion element to which the sample is affixed or as a shift in the mechanical resonance frequency of the element. The torque on a sample typically increases with increasing magnetic field, making this technique well suited to anisotropic samples in modest to large applied fields. Here we present results from submicron micromechanical torsional magnetometers fabricated using semiconductor microprocessing, into which nanometer-scale magnetic systems are integrated. From measurements on 6- and 20-nm-thick samples of the recently fabricated ferromagnetic semiconductor $\text{Ga}_{1-x}\text{Mn}_x\text{As}$,¹ as well as micron-scale Ni control samples, we find our magnetometers have a sensitivity of $3 \times 10^6 \mu_B$ at 0.1 T, and improvement of nearly 5 orders of magnitude upon existing torsional magnetometers. We present measurement of the magnetization, remanent moment, and irreversibility field as a function of temperature for these structures.

Maximizing the sensitivity of a torsional magnetometer requires decreasing the spring constant of the torsion element and increasing its resonant frequency ν_0 . Recent advances in torsional magnetometry,²⁻⁵ even those using semiconductor micromachining,⁶⁻¹⁰ have tended to limit their sensitivities by using a torsion element stiff enough to support large samples. For large samples, a larger, less sensitive magnetometer may be preferable; here we focus on achieving maximum moment sensitivity for small samples. To this end, we fabricate micromechanical cantilevers hundreds of microns long, tens of microns wide, and 100 nm thick. Samples

grown by molecular beam epitaxy (MBE) or evaporative deposition can be integrated into the cantilever structure, using a modified version of a process described previously.¹¹ Starting with the MBE structure shown in Fig. 1(a), the sample layer and top GaAs layer are patterned into mesas which will lie at the ends of the levers. For the $\text{Ga}_{0.962}\text{Mn}_{0.038}\text{As}$ samples 15- μm -radius disks of the $\text{Ga}_{0.962}\text{Mn}_{0.038}\text{As}$ sample layer (which includes a 35- \AA -thick GaAs capping layer) are etched with 1:30 $\text{NH}_4\text{OH}:\text{H}_2\text{O}_2$ ("PA-30", which selectively etches $\text{Ga}_{0.962}\text{Mn}_{0.038}\text{As}$ and GaAs over $\text{Al}_{0.7}\text{Ga}_{0.3}\text{As}$) through a photoresist mask. The exposed $\text{Al}_{0.7}\text{Ga}_{0.3}\text{As}$ is then removed in a $\text{HF}:\text{H}_2\text{O}$ etch. The levers are defined in the middle GaAs layer by a second photoresist mask (which covers the sample mesas) and a PA-30 etch which stops on the lower $\text{Al}_{0.7}\text{Ga}_{0.3}\text{As}$ layer. The back of the chip is patterned with a photoresist mask, and the portion of the substrate under the levers is removed using a

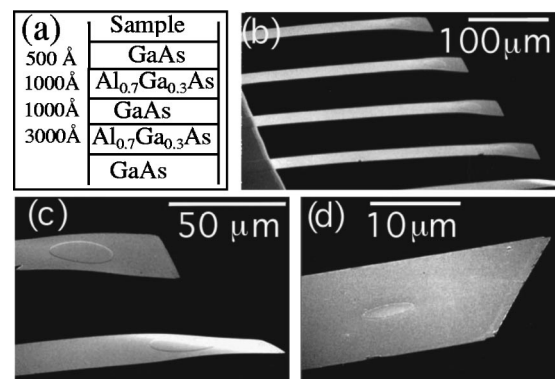


FIG. 1. (a) The MBE growth structure. (b) Five finished cantilevers with 15 μm radius $\text{Ga}_{0.962}\text{Mn}_{0.038}\text{As}$ mesas at their ends. The twist at the very ends of the levers is due to the strain in the $\text{Ga}_{0.962}\text{Mn}_{0.038}\text{As}$. (c) Closeup of the $\text{Ga}_{0.962}\text{Mn}_{0.038}\text{As}$ mesas of the two lowermost levers shown in (b). (d) The end of a GaAs lever on which a 2.5 μm radius Ni disk has been patterned.

^{a)}Electronic mail: awsch@physics.ucsb.edu

PA-30 spray etch, which stops on the lower $\text{Al}_{0.7}\text{Ga}_{0.3}\text{As}$ layer. The lower $\text{Al}_{0.7}\text{Ga}_{0.3}\text{As}$ layer is removed in a $\text{HF}:\text{H}_2\text{O}$ etch, and the structure is extracted from the liquid using a CO_2 critical point drier.

Figure 1(b) shows five completed levers with 20-nm-thick, low-temperature (LT) MBE-grown (growth temperature = 250 °C), $\text{Ga}_{0.962}\text{Mn}_{0.038}\text{As}$ mesas. The levers are all 50 μm wide and 100 nm thick. The longest lever is $\sim 400 \mu\text{m}$ long, with a calculated force spring constant¹² $k = 2 \times 10^{-5}$ N/m, and corresponding torsional spring constant¹³ $\gamma = 2 \times 10^{-12}$ N/m/radian. The levers are quite straight over nearly all of their length, but show a twist of several degrees in their last 50 μm . This is observed in all levers with LT MBE-grown mesas (independent of the presence of Mn), and is attributed to strain due to the $\sim 0.1\%$ lattice mismatch¹⁴ between GaAs and LT GaAs. Levers made out of a continuous sheet of LT $\text{Ga}_{1-x}\text{Mn}_x\text{As}$ show substantial curvature over their entire length. Figure 1(c) is a closeup of the two lowermost levers in Fig. 1(b), showing the two different ways the strain can buckle the levers.

It is possible to replace the patterned sample layer with an evaporation and liftoff step. Figure 1(d) shows the end of a GaAs lever on which a 2.5 μm radius disk of 100-Å-thick Ni on 40-Å-thick Au has been patterned, chosen to give the same magnetic moment at low temperatures as the $\text{Ga}_{0.962}\text{Mn}_{0.038}\text{As}$ mesas in Figs. 1(b) and 1(c). We have also made GaAs levers with mesas of various II–VI heterostructures, using a BCl_3 reactive ion etch to pattern the sample layer.

After fabrication, the lever is mounted in a ^3He cryostat with a 8 T superconducting solenoid with the field normal to the lever. The lever is driven with a piezoelectric crystal, and its displacement detected by a fiber optic interferometer,¹⁵ using a 1310 nm laser diode to avoid creating carriers in the lever. The inset in Fig. 2(a) shows a resonance curve of the lowest flexural mode (the mode used in all the measurements described here) of the lever shown in Fig. 1(d) at 4.3 K and zero applied field. The fit (solid line) to a simple harmonic oscillator gives the quality factor $Q = 11\,500$. Below 5 K all our levers have $10\,000 < Q < 15\,000$ at zero field, independent of their length, which ranges from 150 to 400 μm . Driving the lever in a phase-locked loop, we measure ν_0 to 1.5 parts in 10^6 in a 1 Hz equivalent noise bandwidth using 100 nm vibration amplitude. This limit is due to vibrational noise of the lever, and is consistent with a thermomechanical noise temperature¹⁶ of 4.5 K. We have primarily used the shift in ν_0 to measure magnetization. We can resolve displacements of the lever of 1 nm or better, but this approach tends to be more susceptible to drifts.

The interpretation of shifts in ν_0 for ferromagnetic samples on torsional oscillators in applied fields has been considered for some special cases elsewhere.^{2,17} One first finds the equilibrium orientation of the magnetization $\mathbf{M} = \mathbf{M}_{\text{eq}}$ in a field \mathbf{H} by minimizing the magnetic free energy density

$$G = -\mathbf{M} \cdot \mathbf{H} + f[\mathbf{M}] \quad (1)$$

with respect to \mathbf{M} . $f[\mathbf{M}]$ is the anisotropy energy density and depends upon the orientation of \mathbf{M} relative to some axes fixed to the sample. The torque on a sample of volume V is

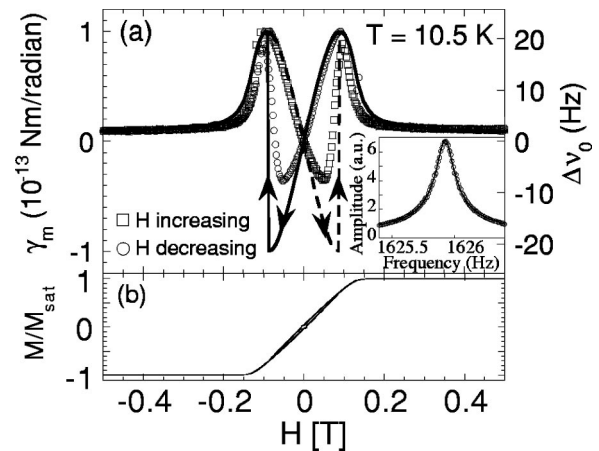


FIG. 2. (a) (Inset) Resonance curve of the lever in Fig. 1(d) at 4.3 K and $H = 0$ T. The solid line is a fit to the data with $Q = 11\,500$. (Main body) Measured shift in spring constant γ_m and resonant frequency ν_0 as function of H at $T = 10.5$ K for one of the levers with a $\text{Ga}_{0.962}\text{Mn}_{0.038}\text{As}$ mesa shown in Fig. 1(b). The solid and dashed lines are simulations of the frequency shift of a cantilever with a ferromagnetic sample attached. (b) The $M(H)$ curve corresponding to the simulation shown in (a) on the same horizontal axis as (a).

then given by $V \partial G[\mathbf{M}_{\text{eq}}] / \partial \theta$, where θ is the lever rotation, and the magnetic contribution to the spring constant $\gamma_m = V \partial^2 G[\mathbf{M}_{\text{eq}}] / \partial \theta^2$. Upon choosing a form for $f[\mathbf{M}]$, Eq. (1) can be solved for γ_m analytically in some cases^{17,18} and numerically otherwise.

For comparison with this model, we measure $\nu_0[H]$ and plot $\gamma_m[H] = \gamma_0((\nu_0[H] / \nu_0[0])^2 - 1)$, where γ_0 is the spring constant at $H = 0$ T. Figure 2(a) shows a measurement of $\gamma_m[H]$ at 10.5 K for a lever with a 20-nm-thick, 15 μm radius $\text{Ga}_{0.962}\text{Mn}_{0.038}\text{As}$ mesa [second from the top in Fig. 1(b)].

We find good agreement between the data in Fig. 2(a) and solutions of Eq. (1) (shown as dashed and solid lines) by assuming a uniaxial form for $f[\mathbf{M}]$ with an easy axis in the plane defined by \mathbf{H} and the torsional axis of the lever and pointing a few degrees above the torsional axis. Since the sample is twisted $\sim 10^\circ$ by the strain (as discussed above), this is consistent with an easy axis in the plane of the $\text{Ga}_{0.962}\text{Mn}_{0.038}\text{As}$ mesa. Figure 2(b) shows the $M[H]$ curve corresponding to this simulation. The data in Fig. 2(a) are in agreement with this model except in the region of the reversal of \mathbf{M} . This discrepancy is probably due to the reversal of \mathbf{M} by some mode other than coherent rotation, such as the formation of domain walls, which is quite likely in a sample this large. This effect would tend to make the reversal of \mathbf{M} take place over a finite field range rather than in a sudden jump, consistent with what we observe in the data. The saturation field we measure at 4.3 K, ~ 0.15 T, is consistent with typical values measured along hard magnetization directions for $\text{Ga}_{1-x}\text{Mn}_x\text{As}$ samples with $x \sim 0.04$.^{19,20}

In a different sample for the same chip, and the Ni sample in Fig. 1(d), we measure a hard axis normal to the sample mesa. While both cases would produce similar $M[H]$ curves, the torsional magnetometer's sensitivity to the orientation of the anisotropy results in a change of sign of γ_m . For the Ni sample, which is polycrystalline and has a much greater moment density than $\text{Ga}_{0.962}\text{Mn}_{0.038}\text{As}$, this orientation is what one would expect from shape anisotropy. The

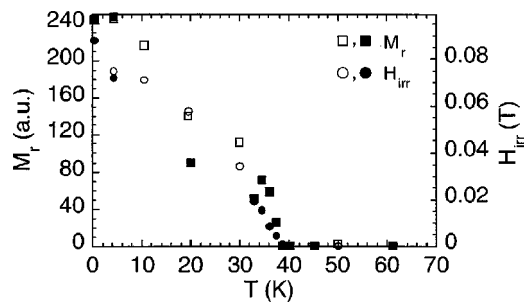


FIG. 3. Temperature dependence of the remanent moment M_r and irreversibility field H_{irr} for two 20-nm-thick $\text{Ga}_{0.962}\text{Mn}_{0.038}\text{As}$ samples. Closed symbols are data from a lever with hard axis normal to the sample plane, and open symbols from a lever with easy axis in the sample plane.

anisotropy in $\text{Ga}_{1-x}\text{Mn}_x\text{As}$, however, is determined largely by strain due to lattice mismatch with the substrate.¹⁹ For thick layers (>100 nm) the anisotropy axis is typically parallel to the growth direction. In samples with multiple thinner (12 nm) layers, angle dependent hysteresis²⁰ shows an in-plane easy axis. The different anisotropies we measure for samples on the same chip may reflect the different ways in which strain is partially released in these suspended structures [Fig. 1(c)].

Measuring $\gamma_m[H]$ for several different temperatures, we find that both the remanent moment M_r and the coercive field vanish above $T_c = 39$ K. Figure 3 shows M_r (which is proportional to the slope of $\gamma_m[H]$ at $H=0$) and H_{irr} , the irreversibility field, as a function temperature. At fields from 0.5 to 8 T, γ_m is constant for $T < 30$ K, indicating that the sample is saturated. Above 30 K, there is an increasing paramagnetic component. Illumination of the sample with a blue light-emitting diode (LED) has no measurable effect on the magnetization of the $\text{Ga}_{0.962}\text{Mn}_{0.038}\text{As}$ either above or below T_c .

We observe peaks in the mechanical dissipation of the levers at fields corresponding to the $\text{Ga}_{0.962}\text{Mn}_{0.038}\text{As}$ saturation field. Dissipation peaks at the saturation field of hard axis samples have previously been attributed to rotational hysteresis due to the oscillator motion,²¹ although this requires rather precise alignment of the hard axis with \mathbf{H} . No such dissipation peaks are seen in the Ni sample.

Measurement on a similar lever with a 6-nm-thick $\text{Ga}_{0.962}\text{Mn}_{0.038}\text{As}$ mesa reveal no ferromagnetism down to 350 mK. Previous measurements using a superconducting quantum interference device magnetometer on multiple layer samples have shown that for a layer thickness less than 7 nm ferromagnetism does not occur above 2 K.²⁰

From the signal to noise ratio of these measurements, we can extract the sensitivity of our magnetometers. The physical quantities which the levers measure are torques (as displacements) and changes in γ (as shifts in ν_0). The relation between these quantities and \mathbf{M} depends upon the anisotropy of the sample and \mathbf{H} . For the levers described above, we resolve changes in ν_0 of 2.6 mHz (changes in γ of 1×10^{-17} N m/radian) in a 1 Hz bandwidth. The total shift in ν_0 of the $\text{Ga}_{0.962}\text{Mn}_{0.038}\text{As}$ samples (which contain 10^{10} Mn ions, giving a maximum estimated moment of $5 \times 10^{10} \mu_B$) is 37 Hz at 4.3 K and 0.1 T. From these values, we find a moment sensitivity of $3 \times 10^6 \mu_B$ at 0.1 T in a 1 Hz bandwidth. For samples with stronger or weaker anisotropies, the

sensitivity will be correspondingly greater or less. The greatest previously reported sensitivity (for a 1 Hz bandwidth, using the ν_0 shift method) of which we are aware is $\sim 10^{-11}$ N m/radian.⁷ For dc torque measurements, moment sensitivities of $\sim 10^{11} \mu_B$ at 0.1 T have been reported.^{5,8,9}

In conclusion, we have developed a fabrication technique to integrate various magnetic samples into micromechanical torsional magnetometers. We detect changes in their spring constants as small as 1×10^{-17} N m/radian in a 1 Hz bandwidth, roughly six orders of magnitude more sensitive than other torsional magnetometers. Measurements on 6- and 20-nm-thick mesas of $\text{Ga}_{0.962}\text{Mn}_{0.038}\text{As}$ integrated into such structures demonstrate a moment sensitivity of $3 \times 10^6 \mu_B$ at 0.1 T in a 1 Hz bandwidth, nearly five orders of magnitude greater than previous torsional magnetometers. These measurements indicate that finite size effects strongly depress the ferromagnetic T_c , and (along with the partial release of strain in the suspended samples) also alter the character of the magnetic anisotropy in this material.

The authors are grateful to N. Samarth and R. Knobel for II–VI MBE growth, and to J. Casey and J. Grimaldi for assistance in developing the cantilever process. Work at Tohoku University is supported by the JSPS Research for the Future Program. This work was supported by AFOSR Grant No. F49620-99-1-0033 and QUEST, the NSF Science and Technology Center for Quantized Electronic Structures, Grant No. DMR91-20007.

¹H. Ohno, *Science* **281**, 951 (1998).

²U. Gradmann, W. Kümmerle, and R. Tham, *Appl. Phys.* **10**, 219 (1976).

³J. P. Eisenstein, *Appl. Phys. Lett.* **46**, 695 (1985).

⁴R. N. Kleiman, P. L. Gammel, E. Bücher, and D. J. Bishop, *Phys. Rev. Lett.* **62**, 328 (1989).

⁵S. A. J. Wiegiers, M. Specht, L. P. Lévy, M. Y. Simmons, D. A. Ritchie, A. Cavanna, B. Etienne, G. Martinez, and P. Wyder, *Phys. Rev. Lett.* **79**, 3238 (1997).

⁶P. L. Gammel, L. F. Schneemeyer, J. V. Waszczak, and D. J. Bishop, *Phys. Rev. Lett.* **61**, 1666 (1988).

⁷P. A. Crowell, A. Madouri, M. Specht, G. Chaboussant, D. Mailly, and L. P. Lévy, *Rev. Sci. Instrum.* **67**, 4161 (1996).

⁸M. Willemin, C. Rossel, J. Brugger, M. H. Despont, H. Rothuizen, P. Vettiger, J. Hofer, and H. Keller, *J. Appl. Phys.* **83**, 1163 (1998).

⁹M. J. Naughton, J. P. Ulmet, A. Narjis, S. Askenazy, M. V. Chaparala, and R. Richter, *Physica B* **246–247**, 125 (1998).

¹⁰V. Aksyuk, F. F. Balakirev, G. S. Boebinger, P. L. Gammel, R. C. Haddon, and D. J. Bishop, *Science* **280**, 720 (1998).

¹¹J. G. E. Harris, D. D. Awschalom, K. D. Maranowski, and A. C. Gossard, *Rev. Sci. Instrum.* **67**, 3591 (1996).

¹²D. Sarid, *Scanning Force Microscopy: With Applications to Electric, Magnetic, and Atomic Forces* (Oxford University Press, New York, 1994), p. 13.

¹³D. A. Walters, J. P. Cleveland, N. H. Thompson, P. K. Hansma, M. A. Wendman, G. Gurley, and V. Elings, *Rev. Sci. Instrum.* **67**, 3583 (1996).

¹⁴J. P. Ibbetson, Ph.D. thesis, University of California at Santa Barbara, 1997.

¹⁵T. R. Albrecht, P. Grütter, D. Rugar, and D. P. E. Smith, *Ultramicroscopy* **42–44**, 1638 (1992).

¹⁶T. R. Albrecht, P. Grütter, D. Horne, and D. Rugar, *J. Appl. Phys.* **69**, 668 (1991).

¹⁷H. J. Elmers and U. Gradmann, *Appl. Phys. A: Solids Surf.* **51**, 255 (1990).

¹⁸J. G. E. Harris and D. D. Awschalom (unpublished).

¹⁹A. Shen, H. Ohno, F. Matsukura, Y. Sugawara, N. Akiba, T. Kuroiwa, A. Oiwa, A. Endo, S. Katsumoto, and Y. Iye, *J. Cryst. Growth* **175–176**, 1069 (1997).

²⁰M. Tanaka, *Physica E* **2**, 372 (1998).

²¹U. Gradmann, *Ann. Phys. (N.Y.)* **17**, 91 (1966).